Dynamics in Carom and Three Cushion Billiards

Inhwan Han*
Department of Mechano-Informatics & Design Engineering, Hongik University, Jochiwon, Choongnam 339-701, Korea

This paper presents the analysis results of dynamics in the billiards game within the framework of rigid-body mechanics and a numerical simulation program. The friction exists between the ball and the table bed as well as between the ball and the rail. There are three parts in the dynamic behavior of the ball on the table bed ; motion of the ball on the table bed, collision between balls, and collision between the ball and the cushion. During the development of the simulation program, the dynamics problems such as rolling motion and three-dimensional frictional impact motion have been analyzed in detail. The theoretical issues are implemented into a viable graphic simulation program and its efficacy is demonstrated through the experimental validation of the billiards game. The resulting analysis results are verified quantitatively and qualitatively using high-speed video camera. Through the experimental tests, it was found that the physical parameters such as coefficients of restitution and friction vary according to the motion variables and corresponding empirical formulations were developed. The simulation and experimental results agree well.

Key Words : Billiards, Rigid-Body Mechanics, Friction, Impact

1. Introduction

Carom billiards is a form of billiards game played on a table without pockets and is dominant in much of Asia, United States and northern European countries. There are 2-4 players (or teams) and the object at each player's turn is to drive the cue ball (white) into both of other object balls (red). In three cushion billiards, the player must hit three or more cushions before hitting the second ball. The cue ball is struck with the cue tip, causing it to hit other balls and cushions. There are wooden surrounds of the rails around the table. Rails are the cushions that mark the field of play. Seven diamonds on the long sides of the table and three on the short sides divide the rails of equal lengths (Cohen, 2002).

Many undergraduate physics and dynamics texts offer billiards dynamics as illustrative examples of rolling and elastic collision mechanics. However, casual observation of such examples shows that billiard balls on real surfaces do not even approximately conform to the results expected from the usual elementary analysis (Wallace and Schroeder, 1988). The theory of billiards is based on rigid-body mechanics (Petit, 2004), and trajectories of balls are mainly influenced by friction and impact phenomena (Cheng et al., 2004). The friction exists between the ball and table bed as well as between the ball and the rail. Usually, the ball rotates with sliding for a time due to the imparted impulses after the strike with the cue tip or the impact, and rolls purely on the table. The ball is generally assumed to have three rotational and two linear velocity components. However, there are two types of impact phenomena except ball-cue tip stroke, ball-ball and ball-rail impacts. As far as the author knows, the

* **E-mail** : ihhan@hongik.ac.kr
TEL : +82-41-860-2581; **FAX** : +82-41-865-9321
Department of Mechano-Informatics & Design Engineering, Hongik University, Jochiwon, Choongnam 339-701, Korea. (Manuscript **Received** November 15, 2004; **Revised** February 21, 2005)

ball-rail impacts have not been analyzed thoroughly while there are extensive works for the collisions between balls (Wallace and Schroeder, 1988; Onoda, 1989). The impact event has been considered as a 3-dimensional problem which differs essentially in some points from the corresponding problems in two dimensions. This paper does not include the analysis results of the ball-cue tip stroke for which the empirical formulation has been performed. Many efforts are concentrated to analyze the frictional impact between the ball and the rail while the ball-ball impact can be easily considered as the impact without friction. This paper presents analytical analysis results for the billiards mechanics in the framework of rigid-body dynamics (Jeong et al., 2003). The theoretical issues are implemented into a viable graphic simulation program and its efficacy is demonstrated through the experimental validation of the billiards game. The resulting analysis results are verified quantitatively and qualitatively using high-speed video camera.

2. Striking the Cue Ball

It is difficult to model analytically and quantitatively the stroke process with the cue because of interposition of a human player. Therefore, the stroke must be modeled qualitatively and empirically for simulation purpose. There are 4 elements that must be considered for striking the cue ball as follows (see Fig. 1).

- Cue points: struck point on the cue ball, divided into 9 different points (C, L, R, F, D, LF, LD, RF, RD)
- Stoke force: amplitude of imparted force
- Stroke method: 3 classified methods (normal shot, draw shot, follow shot)
- Throw direction: direction of stroke (direction of stroke force)

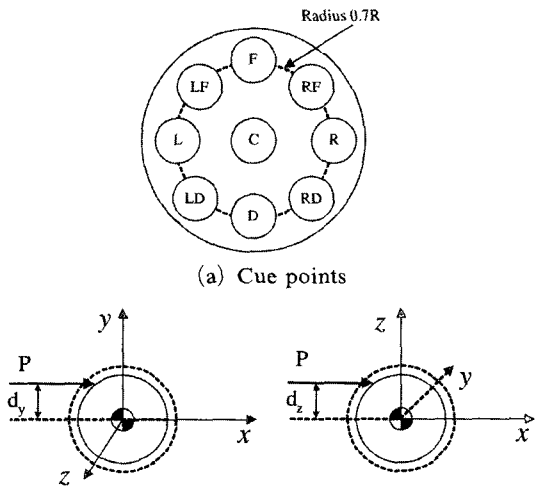

Fig. 1 Cue points and the throw direction

3. Rolling Motion of Balls on the Table

For the movement of a spherical ball over a flat surface, three types of resistive force can be considered. There is a drag force due to the air, a resistive force due to the deformation of the surface and the ball in the contact zone, and eventually a sliding force if the motion is not a pure rolling motion. The air drag force is much smaller than the rolling resistive force for billiards balls (Witters and Duymelinck, 1986). As shown in Fig. 2, the ball on the table has three rotational motion components (ω_X, ω_Y, ω_Z), two sliding motion components (v_X, v_Y), and frictional variables (f_X, f_Y, M_Z). When the ball is struck with the cue tip or hit by other ball, the ball begins to rotate with sliding for a while. The sliding velocity v_a at a contact point a is not zero. Then, the ball finally rolls purely due to friction force on

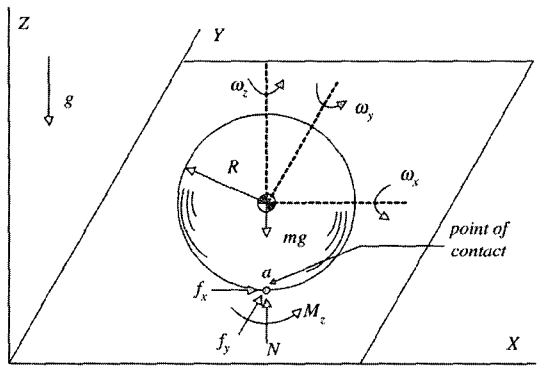

Fig. 2 A ball on the table bed

the table surface unless it hits other ball or rail. In other words, the sliding velocity v_a at a contact point a decreases gradually until the ball hits others and becomes zero. The governing equations of motion for the ball can be written as Eqs. (1) ~ (3).

$$I\omega_X' = Rf_Y,\ I\omega_Y' = -Rf_X,\ I\omega_Z' = -M_Z\frac{\omega_Z}{|\omega_Z|} \quad (1)$$

$$mv_X' = f_X,\ mv_Y' = f_Y \quad (2)$$

$$v_{aX} = v_X - R\omega_Y,\ v_{aY} = v_Y + R\omega_X \quad (3)$$

where,

$$v_Z = v_Z' = 0,\ I = \frac{2}{5}mR^2[=I_{XX}=I_{YY}=I_{ZZ}]$$

In the above equations, f_X, f_Y are frictional forces between the ball and the table surface, and the M_Z is frictional moment. The isotropic Coulomb's frictional forces are shown in Eq. (4).

$$f_X = -f\frac{v_{aX}}{\sqrt{v_{aX}^2+v_{aY}^2}},\ f_Y = -f\frac{v_{aY}}{\sqrt{v_{aX}^2+v_{aY}^2}} \quad (4)$$
$$f = \sqrt{f_X^2+f_Y^2} = \mu mg\ (\mu=\mu_s=\mu_k)$$

The friction moment M_Z should be considered so that diminishing effect of side-spin motion can be modeled. The ball has a surface contact instead of a point contact with the table cloth. However, the contact is assumed as a point contact and the equivalent friction moment is introduced. Fig. 3 shows the contact area of radius ρ with the table surface cloth. The radiusis ρ measured and found to have maximum value of 2 mm. The friction moment M_Z can be expressed as shown in Eq. (5) under the assumption of uniform distribution of the ball weight on the contact area.

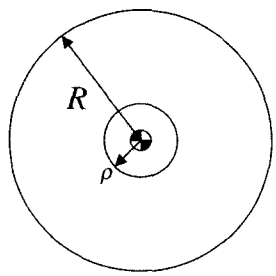

Fig. 3 Contact area of the ball on the surface of table bed

$$M_Z = \int_0^\rho \mu\left(\frac{m}{\pi\rho^2}\right) g(2\pi r dr)\, r$$
$$= \frac{2\mu mg}{\rho^2}\int_0^\rho r^2 dr = \frac{2}{3}\mu mg\,\rho \quad (5)$$
$$M_Z \approx \mu mg\left(\frac{2}{3}\rho\right)\ [=\text{constant}]$$

On the table, the ball can take two different phases of motion, rotating with sliding and pure rolling, respectively. First, the equations of motion during the period of rotating with sliding are shown as Eq. (6).

$$\dot{X}_G = v_X,\ \dot{Y}_G = v_Y$$
$$\dot{v}_X = -\mu g\frac{v_{aX}}{\sqrt{v_{aX}^2+v_{aY}^2}}$$
$$\dot{v}_Y = -\mu g\frac{v_{aY}}{\sqrt{v_{aX}^2+v_{aY}^2}}$$
$$\dot{\omega}_X = -\frac{5}{2}\frac{\mu g}{R}\frac{v_{aY}}{\sqrt{v_{aX}^2+v_{aY}^2}} \quad (6)$$
$$\dot{\omega}_Y = \frac{5}{2}\frac{\mu g}{R}\frac{v_{aX}}{\sqrt{v_{aX}^2+v_{aY}^2}}$$
$$\dot{\omega}_Z = \frac{5}{2}\frac{M_Z}{mR^2}sgn(\omega_Z)$$

When the sliding velocity at contact point a becomes 0, the ball exhibits pure rolling motion and equation of motion can be expressed as Eq. (7).

$$\dot{X}_G = v_X,\ \dot{Y}_G = v_Y$$
$$\dot{v}_X = -\frac{5}{7}\frac{M_Y}{mR}\frac{\omega_Y}{\sqrt{\omega_X^2+\omega_Y^2}}$$
$$\dot{v}_Y = \frac{5}{7}\frac{M_X}{mR}\frac{\omega_X}{\sqrt{\omega_X^2+\omega_Y^2}}$$
$$\dot{\omega}_X = -\frac{5}{7}\frac{M_X}{mR^2}\frac{\omega_X}{\sqrt{\omega_X^2+\omega_Y^2}} \quad (7)$$
$$\dot{\omega}_Y = -\frac{5}{7}\frac{M_Y}{mR^2}\frac{\omega_Y}{\sqrt{\omega_X^2+\omega_Y^2}}$$
$$\dot{\omega}_Z = -\frac{5}{7}\frac{M_Z}{mR^2}\frac{\omega_Z}{\sqrt{\omega_X^2+\omega_Y^2}}$$

In Eq. (7), M_X and M_Y are rotational resistance moments during the pure rolling motion and should be estimated through simulation and experimental tests. The moments are shown in Eq. (8).

$$M_X=M_Y=M_R,\ M_R\leq\frac{7}{5\sqrt{2}}R\mu mg \tag{8}$$

As the motion of the system proceeds, the sliding velocity is monitored. When the velocity approaches zero, the governing equation is changed to Eq. (7) for pure rolling phase from Eq. (6) for rotating with sliding. The information needed to predict the transition time is obtained by monitoring previous values of the sliding velocity at discrete points in time. Then, a numerical root finding method is used to predict the transition time.

4. The Impact Dynamic

In a billiards game, there are two types of impacts, ball-ball and ball-rail impact. The ball-rail impact is treated as an elastic 3-diemensional frictional impact while the ball-ball impact is considered as a smooth impact without friction. In order to simulate the system, the point of contact and time of impact between bodies must be determined. Under the assumption of a rigid body, the problem can be reduced geometrically to determining when one or more points on a body's boundary come into contact with a boundary of another body. In order to predict the time of impact, the relative normal distance and its time derivatives are used. The predicted time is used to estimate a time step such that the colliding bodies will not be allowed to penetrate each other. Control of the simulation time step is continued until either the prediction rules are no longer true or the detection rule becomes satisfied (Han and Gilmore, 1993).

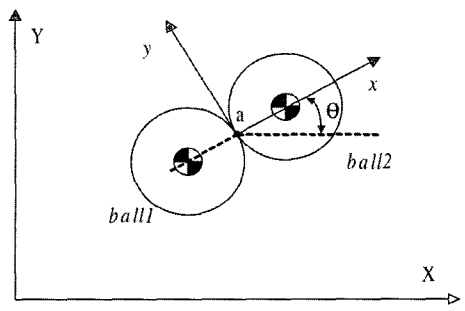

Fig. 4 Impact between balls

The coefficient of restitution between balls e has been measured as 0.98 through preliminary experiments and the frictional effect between balls is negligibly small. For the ball-ball impact shown in Fig. 4, the principle of momentum conservation is expressed as Eq. (9).

$$\begin{aligned} m_1v_{1x}+m_2v_{2x}&=m_1v'_{1x}+m_2v'_{2x}\\ v_{1x}+v_{2x}&=v'_{1x}+v'_{2x}\end{aligned} \tag{9}$$

Newton's hypothesis gives the kinematic relationship shown in Eq. (10).

$$e(v_{a1x}-v_{a2x})=(v'_{a2x}-v'_{a1x}) \tag{10}$$

Then, the velocity v_{ax} at a contact point equals to the velocity v_x of the center of the billiard ball.

From Eq. (9) and (10), the post-impact velocities of balls are obtained as Eq. (11).

$$\begin{aligned} v'_{1x}&=\frac{1-e}{2}v_{1x}+\frac{1+e}{2}v_{2x}\\ v'_{2x}&=\frac{1+e}{2}v_{1x}+\frac{1-e}{2}v_{2x}\end{aligned} \tag{11}$$

Here, v_y, ω_x, ω_y, ω_z don't change after collision since there is no friction between balls.

However, the actual physical process of ball-rail impact is highly complex. In order to render the problem amenable to mathematical treatment some simplifying assumptions must be made. In rigid body mechanics impact is treated as instantaneous. This research does not assume that impact is instantaneous, but that its duration is small compared to a typical time scale before or after the impact. Therefore, it is assumed that during the small time interval the positions and angular orientations of all bodies remain unchanged, since all velocities remain finite. Another assumption is that the impact occurs at a point on each rigid body. In fact, all impact forces occur over a surface. This research deals only with point impacts. Fig. 5 shows the configuration of typical ball-rail impact. In Fig. 5, the distance (ε=9.25 mm) between the contact point and the center of ball is assumed to be constant. At any time during the small impact period, the motion of the bodies is governed by linear and angular impulse-momentum laws, which provide the following Eq. (12) and (13).

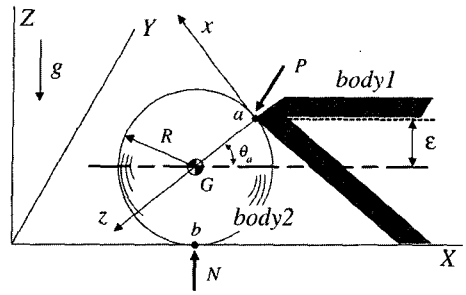

Fig. 5 Impact between the ball and the cushion rail

$$m(v_X-v_{X0})=P_X,\ m(v_Y-v_{Y0})=P_Y$$
$$m(v_Z-v_{Z0})=P_Z+N=0 \text{ or } P_Z=-N \quad (12)$$
$$I(\omega_X-\omega_{X0})=-RP_Y\sin\theta_a$$
$$I(\omega_Y-\omega_{Y0})=RP_X\sin\theta_a-RP_Z\cos\theta_a \quad (13)$$
$$I(\omega_Z-\omega_{Z0})=RP_Y\cos\theta_a$$

The relative velocities of sliding and compression of the points in contact are given by Eq. (14)

$$s_x=-v_{ax}=v_X\sin\theta_a-v_Z\cos\theta_a+R\omega_Y$$
$$s_y=-v_{ay}=-v_Y-R\omega_Z\cos\theta_a+R\omega_X\sin\theta_a \quad (14)$$
$$c=-v_X\cos\theta_a-v_Z\sin\theta_a$$

Using Eq. (12) and (13), Eq. (14) can be restated as Eq. (15) in terms of impulse and momentum.

$$s_x=s_{x0}-AP_x,\ s_y=s_{y0}-A'P_y$$
$$c=c_0-BP_z \quad (15)$$

where

$$s_0=s(t_0),\ c_0=c(t_0)$$
$$A=A'=\frac{1}{m}+\frac{R^2}{I}=\frac{7}{2m}\quad B=\frac{1}{m} \quad (16)$$

The three constants A, A', B are independent of the initial velocities, but depend on the mass of impacting bodies. For the ball to collide with the rail at a given point, the relative normal velocity c_0 must be positive. In Fig. 5, the 3-dimensional frictional impact analysis is performed for a contact point a and the post-impact velocity along the normal direction to the table surface v_Z' equals to zero because of normal reaction force at contact point b.

There are two possible cases of the 3-dimensional impact process for the ball-rail impact: one is sliding and sticking impact (CASE 1-1) and the other is forward sliding impact (CASE 1-2) (see Han and Cho (1996) or Routh (1891) for more detail of the 3-dimensional impact analysis, and consult with Han and Gilmore (1993) for general analysis of the frictional impact dynamics). For both cases, the normal impulse through out the impact process is shown in Eq. (17).

$$P_{zE}=(1+e)\frac{c_0}{B} \quad (17)$$

The tangential impulses throughout the impact for both cases are calculated as follows.

(CASE 1-1) Sliding and Sticking: $P_{zs}\le P_{zE}$

$$P_{xE}=\frac{s_{x0}}{A},\ P_{yE}=\frac{s_{y0}}{A} \quad (18)$$

(CASE 1-2) Forward Sliding: $P_{zs}>P_{zE}$

$$P_{xE}=\mu(1+e)\frac{c_0}{B}\cos\theta_0$$
$$P_{yE}=\mu(1+e)\frac{c_0}{B}\sin\theta_0 \quad (19)$$

where

$$P_{zs}=\frac{|s_0|}{A} \quad (20)$$

For the sliding and sticking impact (CASE 1-1), the impulses along the fixed coordinate on the table surface can be obtained as Eq. (21),

$$P_X'=-\frac{s_{x0}}{A}\sin\theta_a-(1+e)\frac{c_0}{B}\sin\theta_a$$
$$P_Y'=\frac{s_{y0}}{A} \quad (21)$$
$$P_Z'=\frac{s_{x0}}{A}\cos\theta_a-(1+e)\frac{c_0}{B}\sin\theta_a$$

and Eq. (22) holds for the forward sliding impact (CASE 1-2).

$$P_X'=-\mu(1+e)\frac{c_0}{B}\cos\theta_0\sin\theta_a-(1+e)\frac{c_0}{B}\cos\theta_a$$
$$P_Y'=\mu(1+e)\frac{c_0}{B}\sin\theta_0 \quad (22)$$
$$P_Z'=\mu(1+e)\frac{c_0}{B}\cos\theta_0\cos\theta_a-(1+e)\frac{c_0}{B}\sin\theta_a$$

From Eq. (12) and (13), the post-impact velocities of the ball can be expressed as Eq. (23).

$$v'_X = v_{X0} + \frac{P_X}{m},\quad v'_Y = v_{Y0} + \frac{P_Y}{m}$$
$$\omega_X = \omega_{X0} - \frac{R}{I} P_Y \sin\theta_a$$
$$\omega_Y = \omega_{Y0} + \frac{R}{I}(P_X \sin\theta_a - P_Z \cos\theta_a) \tag{23}$$
$$\omega_Z = \omega_{Z0} + \frac{R}{I} P_Y \cos\theta_a$$

Substituting the expressions for impulses from Eq. (21) or (22) into Eq. (23), the post-impact velocities of the ball are obtained as Eq. (24) and (25).

(CASE 1-1) Sliding and Sticking:

$$v'_X = v_{X0} - v_{X0}\left[\frac{2}{7}\sin^2\theta_a + (1+e)\cos^2\theta_a\right] - \frac{2}{7} R\omega_{Y0}\sin\theta_a \tag{24}$$
$$v'_Y = \frac{5}{7} v_{Y0} + \frac{2}{7} R[\omega_{X0}\sin\theta_a - \omega_{Z0}\cos\theta_a]$$

(CASE 1-2) Forward Sliding:

$$v'_X = v_{X0} - v_{X0}(1+e)\cos\theta_a(\mu\cos\theta_a\sin\theta_a + \cos\theta_a)$$
$$v'_Y = v_{Y0} + \mu(1+e)\cos\theta_a\sin\theta_a v_{X0} \tag{25}$$

As shown in Eq. (24), v'_Y depends on side spin ω_{X0} while v'_X heavily depends on the top spin ω_{Y0} for the sliding and sticking impact. It is interesting that the post impact horizontal velocity v'_Y are independent of physical parameters such as coefficients of restitution and friction. On the other hand, the post-impact velocities for the forward sliding impact are independent of rotational velocities.

5. Simulation and Experimental Tests

All the issues discussed were implemented into a computer graphic simulation system. The fully developed simulation system was tested with

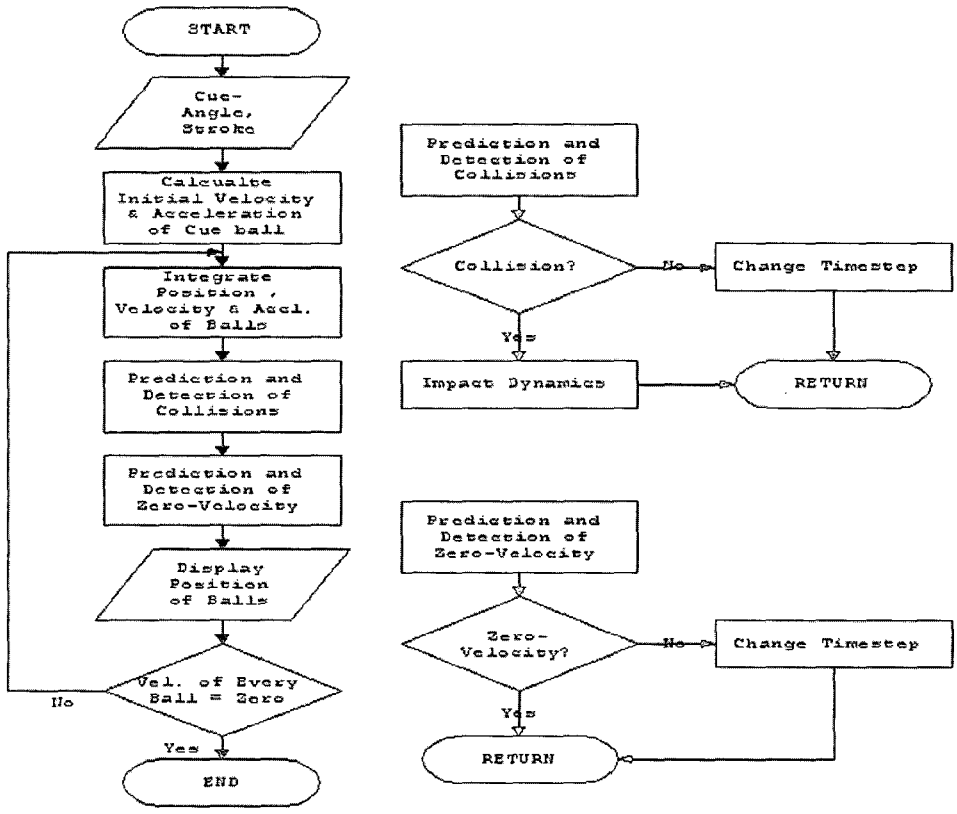

Fig. 6 Flow-chart of the developed simulation system

Table 1 Measured physical parameters in the billiards

Parameters	Value	Parameters	Value
Coeff. of restitution between balls	0.98	Coeff. of friction between ball and table bed	0.069
Coeff. of restitution between ball and rail	0.6~0.95	Coeff. of friction between ball and rail	0.1~0.35
Frictional moment M_z	3.82E-4 (Nm)	M_R $(=M_x=M_y)$	3.8E-4 (Nm)

many example trials of billiards game. The simulation system is composed of following 8 modules which has been developed whenever each issue was addressed and answered. Fig. 6 illustrates the basic structure of the simulation system.

- Striking the cue ball : cue points, amplitude of imparted stroke force, stroke method, throw direction
- Rolling motion of balls on the table surface (Eq. (6) and (7))
- Detection of ball-ball impact
- Detection of ball-rail impact
- Analysis of ball-ball impact : 3-dim. impact without friction (Eq. (11))
- Analysis of ball-rail impact : 3-dim. impact with friction (Eq. (21) and (23) or Eq. (22) and (23))
- Control of simulation time step
- Prediction and detection of time instant when the ball stops motion

In Carom and three cushion billiards, the diameter of the ball is 65.5 mm and the mass is 230 g. The length of long and short rails is 2540 mm and 1270 mm, respectively. In additions, the measured physical parameters through preliminary experimental tests are summarized in Table 1.

The experimental results indicated that the coefficient of restitution varies according to the normal velocity V_{x0} (m/s) of the ball to the rail. The empirical relationship between e and V_{x0} is approximated by Eq. (26).

$$e=0.39+0.257\,V_{x0}-0.044\,V_{x0}^2 \qquad (26)$$

The test results indicated that the friction coefficient between the ball and rail μ varies according to the incidence angle θ(rad). However,

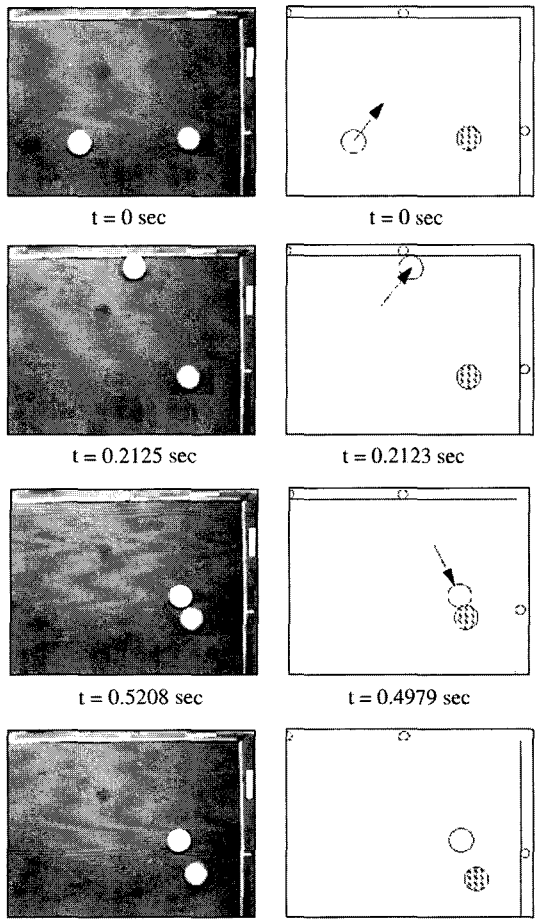

(a) Experimental (b) Simulation

Fig. 7 Experimental and simulation results : one cushion play

there seems to be no clear relationship between μ and V_{X0}. Eq. (27) shows the relationship between and μ θ.

$$\mu=0.471-0.241\times\theta \qquad (27)$$

The above two empirical equations for estimating

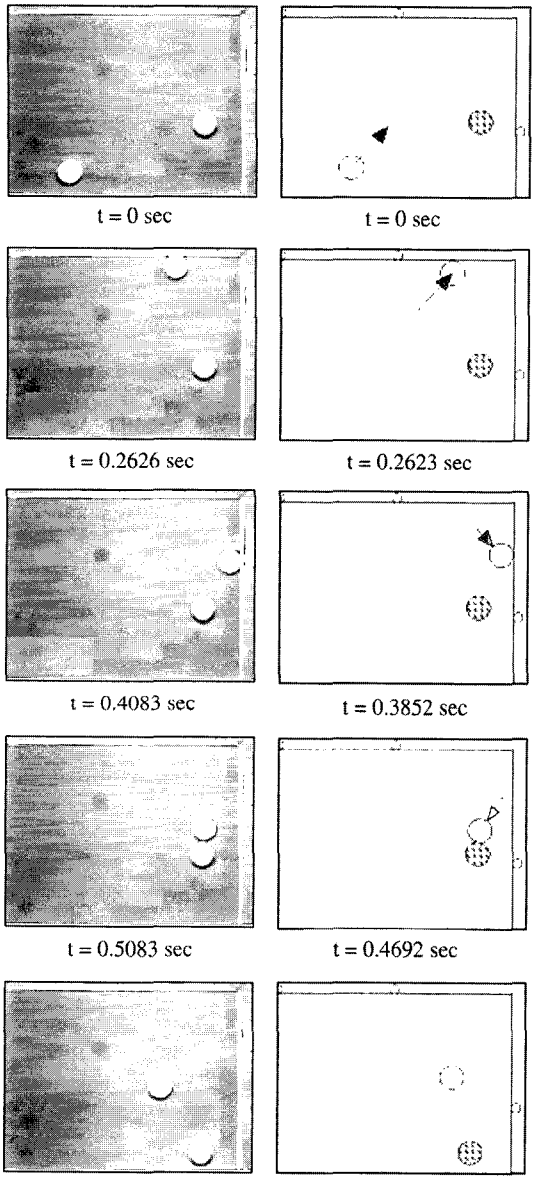

(a) Experimental (b) Simulation

Fig. 8 Experimental and simulation results: two cushion play

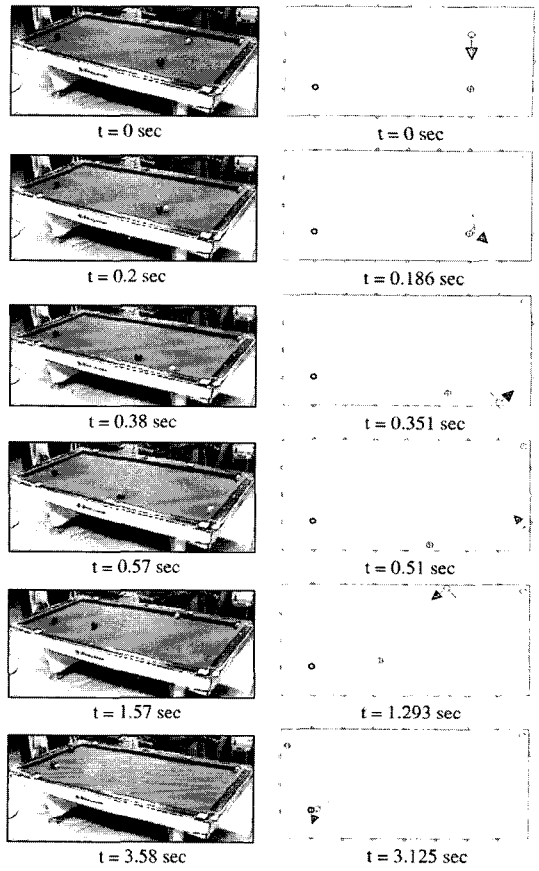

(a) Experimental (b) Simulation

Fig. 9 Experimental and simulation results: three cushion play

coefficients of restitution and friction were derived using the least square curve fitting method with many experimental data.

Experiments are presented for validation of the simulation algorithms. The experiments included one cushion play, two cushion play and three cushion billiards game. The motion of balls was recorded using FASTCAM-Rabbit high speed video camera, capable of 600 frames per second. The recorded video was analyzed frame-by-frame and compared to the numerical output and graphical output which illustrates the simulated motion of balls, thus allowing for validation. Figs. 7 and 8 show examples of one cushion and two cushion play, respectively. The simulation results agree well with the experimental result. However, the slight differences in results might come from the assumption of rigid body for the deformable rail and uncertainties of physical parameters. Fig. 9 shows an example of three cushion play. As shown in Fig. 9, the experimental results agree fairly with the simulation result for the locations of collision points on rails as well as entire motion of balls.

6. Conclusions

This paper presents the analysis of dynamics of billiards game in the framework of rigid body mechanics and the developed numerical simulation program. There are three parts in the dynamic behavior; motion of balls on the bed of table, impacts between balls, and impacts between the ball and the cushion rail. During the development of the simulation program, the dynamics problems such as rolling motion and three-dimensional frictional impact, have been analyzed in detail. The problem of determining the 3-dimensional motion of any two rough bodies after a collision involves some rather long analysis and yet in some points it differs essentially from the corresponding problem in two dimensions. The analytical and numerical results were verified quantitatively and qualitatively through experimental tests using a high-speed video camera. Through the experimental tests, it was found that the physical parameters such as coefficients of restitution and friction vary according to the motion variables and corresponding empirical formulations were developed. The simulation and experimental results agree well.

References

Cheng, B. -R., Li, J. -T. and Yang, J. -S., 2004, "Design of the Neural-fuzzy Compensator for a Billiard Robot," *Proc. of IEEE Int'l Conf. on Networking, Sensing and Control*, Taipei, Taiwan.

Cohen, G. L., 2002, "Three Cushion Billiards : Notes on the Diamond System," *Sports Engineering*, Vol. 5, pp. 43~51.

Han, I. and Gilmore, B. J., 1993, "Multi-body Impact Motion with Friction-Analysis, Simulation and Experimental Validation," *ASME Trans. Journal of Mechanical Design*, Vol. 115, pp. 412~422.

Han, I. and Cho, J., 1996, "Analysis of Three-dimensional Rigid-body Collisions with Friction-Collisions Between Ellipsoids (in Korean)," *Trans. of the Korean Society of Mechanical Engineers*, Vol. 20, No. 5, pp. 1486~1497.

Jeong, M. -Y. et al., 2003, "Chaotic Behavior on Rocking Vibration of Rigid Body Block Structure under Two-dimensional Sinusoidal Excitation," *KSME International Journal*, Vol. 17, No. 9, pp. 1249~1260.

Onoda, G. Y., 1989, "Comment on "Analysis of billiard ball collisions in two dimensions," by R. E. Wallace and M.C. Schroeder [Am. J. Phys. 56, 815-819 (1988)]," *Am J. Phys.*, Vol. 57, No. 5, pp. 476~478.

Petit, R., 2004, "The Art of Billiards Play," http://vrbilliard.tripod.com/practice.html.

Routh, E. J., 1891, *Dynamics of a System of Rigid Bodies*, MacMillan and Co., London, pp. 265~269.

Wallace, R. E. and Schroeder, M. C., 1988, "Analysis of Billiard Ball Collisions in Two Dimensions," *Am. J. Phys.*, Vol. 56, No. 9, pp. 815~819.

Witters, J. and Duymelinck, D., 1986, "Rolling and Sliding Resistive Forces on Balls Moving on a Flat Surface," *Am. J. Phys.*, Vol. 54, No. 1, pp. 80~83.

_____, "All About Billiards," http://allsportsbid.com.